

1  
2  
3  
4  
5  
6  
7  
8  
9  
10  
11  
12  
13  
14  
15  
16  
17  
18  
19  
20  
21

**18 March 2020**

**Role of meteorological temperature and relative humidity in the January-February 2020  
propagation of 2019-nCoV in Wuhan, China**

Jose Alvarez-Ramirez\* and Monica Meraz

Universidad Autónoma Metropolitana-Iztapalapa

Apartado Postal 55-534

Iztapalapa, CDMX, 09340 México

[jjar@xanum.uam.mx](mailto:jjar@xanum.uam.mx)

22

23

24

25

26

27

28

### Abstract

29 Identified in December 2019, the 2019-nCoV emerged in Wuhan, China, and its spread increased  
30 rapidly, with cases arising across Mainland China and several other countries. By January 2020, the  
31 potential risks imposed by 2019-nCoV in human health and economical activity were promptly  
32 highlighted. Considerable efforts have been devoted for understanding the transmission  
33 mechanisms aimed to pursue public policies oriented to mitigate the number of infected and deaths.  
34 An important question requiring some attention is the role of meteorological variables (e.g.,  
35 temperature and humidity) in the 2019-nCoV transmission. Correlations between meteorological  
36 temperature and relative humidity with the number of daily confirmed cases were explored in this  
37 work for the epicenter city of Wuhan, China for the period from 29 January to March 6, 2020.  
38 Long-term trend of temperature and relative humidity was obtained with a 14-days adjacent-  
39 averaging filter, and lagged correlations of the number of daily confirmed cases were explored. The  
40 analysis showed negative correlations between temperatures with the number of daily confirmed  
41 cases. Maximum correlations were found for 6-day lagged temperatures, which is likely reflecting  
42 the incubation period of the virus. It was postulated that the indoor crowding effect is responsible of  
43 the high incidence of 2019-nCoV cases, where low absolute humidity and close human contact  
44 facilitate the transport of aerosol droplets.

45 **Keywords:** 2019-nCoV; temperature; relative humidity; correlations.

46

47

48

## 49 **1. Introduction**

50 Starting in December 2019, a group of patients with pneumonia of unknown origin was found in  
51 Wuhan, China. The illness was linked to a previously unknown coronavirus, which was named  
52 2019-nCoV (Zhu et al., 2020). In the early days of 2020, the WHO alerted on the potential capacity  
53 of the new coronavirus to pose international threatens to human health and global economy. By the  
54 end of January 2020, Wuhan, China was positioned as the epicenter of the 2019-nCoV contagion  
55 and spreading. In January 31, the number of confirmed cases ascended to about 11950, most of  
56 them located in mainland China. Promptly, the coronavirus spread from China to many countries,  
57 with about 75 countries reporting confirmed cases. By March 7, the number of confirmed and death  
58 cases was about 105,782 and 3,569, respectively.

59 The availability of the first set of data on the number of detected infected and death cases  
60 prompted the early characterization of the propagation dynamics. Zhao et al. (2020) reported the  
61 estimated reproduction number  $R_0$  ranging from 2.24 to 3.58 for the early outbreak phase.  
62 Subsequently, Hu et al. (2020) reported the estimated reproduction number 2.68 as of January, 25.  
63 Backer et al. (2020) estimated a mean incubation period of 6.4 days. Overall, reports have shown  
64 that the 2019-nCoV may have a higher pandemic risk than SARS broken out in 2003. Given the  
65 lack of an effective vaccine for controlling the disease, some operational strategies have been  
66 envisioned. Tang et al. (2020) used mathematical modeling contrasted to available data (January  
67 29) to suggest that the best measure for reproduction number reduction is persistent and strict self-  
68 isolation. However, it has been highlighted that isolation strategies have negative effects in the  
69 economic activity, an effect that most governments are reticent to implement, mainly in regions  
70 with strong manufacturing activity.

71 A growing belief, mainly in social networks, is that the 2019-nCoV infection shares some  
72 similarities with seasonal flu, and as such the advent of warmer wheatear would weak propagation  
73 and fatalities. The motivation behind this folk argument is that influenza epidemic events exhibit  
74 wintertime seasonality, with most cases occurring over 2-3 month period between November and  
75 March in Northern Hemisphere, and May and September in Southern Hemisphere (Tamerius et al.,  
76 2013). Formally, the problem is linked to the role of humidity and temperature in the dynamics of  
77 influenza propagation (Lowen and Steel, 2014). Results in this line are still scare, although some  
78 reports have pointed out that the transmission of influenza virus is sensible to temperature and  
79 humidity (Steel, 2011). Experimental runs on transmission at low (5 °C) versus intermediate (20  
80 °C) temperatures were performed with two influenza B viruses, finding that transmission is more  
81 efficient under colder conditions (Pica et al., 2012). It was postulated that transmission of human

82 influenza viruses via respiratory droplet or environment aerosols proceeds most efficiently under  
83 cold, dry conditions. Also, the analysis of laboratory and epidemiological data has provided further  
84 evidence that temperature plays an important role in the transmission efficiency of influenza viruses  
85 (Pica and Bouvier, 2014). Recently, it was found that low humidity and temperature are linked to  
86 seasonal influenza activity in the Toronto area (Peci et al., 2019).

87 Given the potential high risk of the 2019-nCoV, predicting the transmission mechanisms is of  
88 prime importance for the timing of implementation of disease prevention and control measures as  
89 well as for medical resource allocation (Peci et al., 2019). In this regard, the aim of the present  
90 study is to explore the role of environmental factors (temperature and humidity) on the 2019-nCoV  
91 activity in Wuhan, china, from 29 January to 6 March, 2020. The present study was motivated by  
92 the recent report by Wang et al. (2020), who studied the effect of temperature in the transmission  
93 rate of 2019-nCoV and found that every 1 °C increase in the minimum meteorological temperature  
94 led to a decrease of the cumulative number of cases by a factor of about 0.86.

95

## 96 **2. Data sources and methodology**

97 Median temperature and relative humidity (RH) data were obtained from the publicly accessible  
98 website [www.timeanddate.com/weather/china/wuhan](http://www.timeanddate.com/weather/china/wuhan). Data is reported every 6 hours, and mean  
99 daily values were obtained by averaging for the four daily values. On the other hand, number of  
100 daily new cases and deaths were obtained from the official reports by the Hubei Province Minister  
101 of Health at the website <http://wjw.hubei.gov.cn>. Although official reports are available from 23  
102 January, detailed reports for the Hubei Province are given from 29 January.

103 The aim of the analysis is to detect co-movements between the number of daily confirmed cases  
104 and meteorological variables (temperature and relative humidity). To this end, the estimation of a  
105 correlation coefficient will be used to quantify co-movement between two time series. However,  
106 since the daily confirmed cases of 2019-nCoV underwent an incubation period (typically 6-8 days),  
107 the analysis of co-movement might be biased by lagged effects. In this way, the analysis will be  
108 based on the computation of the lagged height cross-correlation analysis (Wang et al., 2016).  
109 Briefly, for two time series  $\{x_t\}$  and  $\{y_t\}$ ,  $t=1, \dots, N$ , the associated accumulation deviation series  
110 are given by

$$\begin{aligned} X(t) &= \sum_{i=1}^t (x_i - \langle x \rangle) \\ Y(t) &= \sum_{i=1}^t (y_i - \langle y \rangle) \end{aligned} \tag{1}$$

112 Here,  $\langle \cdot \rangle$  denotes mean values. The cross increment of these time series with interval  $L$  is  
113 computed as

$$114 \quad F_{XY}(\tau, L)^2 = [X(t) - X(t-L)][Y(t) - Y(t-L-\tau)] \quad (2)$$

115 where  $\tau$  denotes the lag. The lagged correlation coefficient is given by

$$116 \quad \rho(\tau, L) = \frac{F_{XY}(\tau, L)^2}{\sqrt{F_{XX}(\tau, L)^2 F_{YY}(\tau, L)^2}} \quad (3)$$

117 In this way,  $\rho(\tau, L) \in [-1, 1]$ , with negative values for anti-correlations, and positive values for  
118 correlations. It is noted that the analysis is similar to the lagged-DCCA reported by [Shen et al.](#)  
119 [\(2015\)](#) for two time series. Given the relatively low number of data, the computations should use  
120 the scale  $L = N$ . That is, the scrutinized scale corresponds to the number of days from 29 January  
121 to 6 March.

122

### 123 **3. Winter meteorological conditions**

124 Wuhan in mainland China is a metropolis (about 11 millions population), polluted by the intense  
125 industrial activity. Climate in Wuhan is temperate, with relatively cold winters. Commonly, cold air  
126 can stagnate on the ground. There may be cold periods during which the temperature remains  
127 around freezing even during the day, and even snow can fall. Mean min-max temperatures of the  
128 winter season are 3-11 °C for December, 1-8 °C for January, 4-11 °C for February and 7-15 °C for  
129 March. Figures 1.a and 1.b present respectively the behavior of the temperature and relative  
130 humidity for the period from January 1<sup>st</sup>, 2020 (day 1) to date. The mean values of temperature and  
131 relative humidity in the period are  $7.20 \pm 3.85$  °C and  $78.79 \pm 11.68\%$ , respectively. The temperature  
132 dynamics exhibits a pattern composed by large oscillations of mean period of about 10 days, and a  
133 long-term ascending trend. Similar pattern is presented by the relative humidity dynamics, although  
134 the large oscillation has a period of about 15 days. Figure 1.c shows that temperature and relative  
135 humidity are weakly negatively correlated ( $\rho = -0.42$ ).

136

### 137 **4. Dynamics of daily confirmed cases and deaths**

138 Figure 2.a shows the dynamics of the daily confirmed cases ( $C_t$ ) and deaths ( $D_t$ ) for the period from  
139 29 January to 6 March 2020. A large peak in both new cases and deaths at February 12 is exhibited,  
140 which corresponds to an improvement of the classification method, when the number of clinically  
141 confirmed cases was incorporated to the number of new cases. The new cases showed a positive  
142 trend up to February 18, when it presented an important decrease. The behavior of the deaths was

143 similar, although the positive trend was maintained until 23 February. Afterwards, the number of  
144 daily deaths has decreased from values of about 100-120 to about 20-30. Figure 2.b shows the plot  
145 of the number of deaths ( $D_t$ ) and the number of daily confirmed cases ( $C_t$ ). The correlations  
146 between these two variables is positive ( $\rho=0.72$ ), a result that can be expected. However, a stronger  
147 correlation ( $\rho=0.85$ ) is exhibited between the number of actual deaths ( $D_t$ ) and the number of  
148 confirmed cases lagged by 5 days ( $C_{t-5}$ ). The lag of 5 days could be reflecting the mean period  
149 between the clinical diagnostic and the death of seriously illness patients. The continuous line in  
150 Figure 2.c denotes the least-squares fitting by a quadratic function, where a weak convexity can be  
151 observed. This suggests that an increasing number of confirmed cases does not lead linearly to an  
152 increasing number of deaths. Figure 2.d shows the correlation coefficient as function of the lag,  
153 confirming that maximum linear correlations are exhibited for a lag of about 5 days.

154

### 155 **5. Role of temperature and relative humidity**

156 Possible patterns between temperature/relative humidity and the number of new infected cases are  
157 explored next. Figure 3.a shows the behavior of the daily confirmed cases ( $C_t$ ) with respect to the  
158 temperature ( $T_t$ ). No discernible regular pattern between the daily confirmed cases and temperature  
159 can be observed. The correlation coefficient is very low ( $\rho = -0.18$ ), reflecting weak negative trend.  
160 Similar behavior was exhibited by the new cases with respect to the relative humidity ( $RH_t$ ) in  
161 Figure 3.b. In this case,  $\rho = +0.17$ , indicating the presence of weak positive correlations. Figures 3.c  
162 and 3.d present the behavior of the correlation coefficient with respect to the lag for temperature  
163 and relative humidity, respectively. Correlations for temperature are negative, with a peak at about  
164 6-7 days. In contrast, correlations for relative humidity are positive, with two prominent peaks at  
165 about 3 and 8 days. Nevertheless, the magnitude of the correlations is relative small for both cases.  
166 Overall, the results in Figures 3 suggest that no apparent regular pattern is present in the joined  
167 dynamics of new infected cases and meteorological variables (temperature and relative humidity).  
168 In the face of this feature, a different strategy was pursued. A key observation is that the  
169 meteorological variables showed large fluctuations along a secular trend (see Figure 1). Today  
170 confirmed cases correspond to infected cases in past days. It has been reported that the incubation  
171 period of COV-19 is typically 7-14 days, and could be as long as 27 days. In this regard, the effects  
172 of temperature in today confirmed cases are not pointwise, but distributed along several past days.  
173 That is, the dynamical behavior of today confirmed cases is likely to be affected by the temperature  
174 trend in the past few days. The proposed strategy consists in considering the secular trend of the  
175 temperature and relative humidity dynamics, and to search patterns with respect to lagged values.

176 Figures 4.a and 4.b present respectively the long-term trend of temperature and relative humidity,  
177 which were obtained by means of a 14<sup>th</sup>-order moving-average filtering. From January 10, the  
178 temperature showed a positive trend, until February 28 when the trend was negative. The trend  
179 temperature goes from about 4-5 °C by January 10, to about 10-11 °C by February 24. In contrast,  
180 the relative humidity showed a negative trend, until February 24 when the trend was positive.  
181 Figure 4.c compares the trends of temperature and relative humidity, showing an apparent negative  
182 correlation ( $\rho = 0.81$ ) between these two signals. That is, the increase of temperature was  
183 accompanied by a decrease of the relative humidity.

184 Figures 5.a and 5.b present the behavior of the correlation coefficient with respect to the lag for  
185 temperature and relative humidity, respectively. A pattern is more discernible than in figures 3.c  
186 and 3.d, indicating that the use of temperature trend instead of daily temperature is more appropriate  
187 for the analysis of correlations between daily confirmed cases and meteorological variables. The  
188 correlation coefficient for temperature is negative and its magnitude achieved a maximum ( $\rho = -$   
189  $0.77$ ) at about 6 days. The correlation coefficient for relative humidity is positive and S-shaped,  
190 achieving the maximum value ( $\rho = + 0.65$ ) at about 6-7 days. For the lag where maximum  
191 correlations were detected, figures 5.c and 5.d show the plot of the number of daily confirmed cases  
192 versus trend temperature and relative humidity, respectively. This result indicates that the today  
193 number of daily confirmed cases is correlated with the temperature and relative humidity lagged  
194 about one week. The lag of 6-7 days could correspond to the mean incubation period (Tian et al.,  
195 2020). The pattern displayed by temperature in Figure 5.c is interesting. The continuous line depicts  
196 the least-squares sigmoid fitting, which shows a sharp transition from high to low number of daily  
197 confirmed cases. Relative to the 6-days lagged trend temperature, the number of daily confirmed  
198 cases shows two phases with crossover temperature of about 8.6 °C. Below this temperature, the  
199 mean number of daily confirmed cases is about 1635 per day, and above such temperature value the  
200 number of daily confirmed cases decreased to about 360 per day. Overall, the results described in  
201 Figure 5 are in line with a recent report by Wang et al. (2020), who found that the 1 °C increase in  
202 the minimum meteorological temperature led to a decrease of the cumulative number of cases by  
203 0.86 in 429 studied cities.

204

## 205 **6. Discussion**

206 Figure 5.c showed the presence of a marked pattern between the daily confirmed cases and 6-days  
207 lagged temperature trend. In turn, this shows that environmental temperature plays an important  
208 play in the transmission dynamics of 2019-nCoV in Wuhan, China. The 6-7 days period in the

209 temperature lag is likely reflecting the mean incubation period of the virus (Backer et al., 2020). On  
210 the other hand, the two-phase pattern of the number of daily confirmed cases showed that a large  
211 incidence of daily confirmed cases (about 1650 per day) occurred for low environment temperatures  
212 (lower than about 8 °C). Sajadi et al. (2020) reported that 2019-nCoV spread is persistent in cities  
213 and regions along a 30-50° N' corridor showing consistent meteorological conditions with average  
214 temperatures of 5-11 °C, combined with low specific (3-6 g/kg) and absolute humidity (4-7 g/m<sup>3</sup>).  
215 Also, Wang et al. (2020) reported that 1 °C increase in temperature and 1% increase in relative  
216 humidity lower the effective reproduction number by 0.0383 and 0.0224, respectively.

217 A sharp decrease of the number of daily confirmed cases (from about 1800 to about 350 cases  
218 per day) was observed for higher temperatures. Oliveiros et al. (2020) found that the doubling time  
219 of newly confirmed cases has positive correlation with temperature and negative with humidity. In  
220 turn, this suggests a decrease in the rate of transmission of 2019-nCoV with spring and summer  
221 arrivals in the North Hemisphere. The important reduction of the number of new cases is not  
222 necessarily indicating that the virus stability is sensible to relatively high temperatures, but that the  
223 human transmission network is affected by the environment temperature. It is likely that the sharp  
224 transition in Figure 5.c is reflecting the so-called indoor crowding effect. Average low outdoor  
225 temperatures result commonly in indoor crowding as people activities takes place primordially in,  
226 e.g., homes, commercial malls, sport events, and cinema, where temperature is regulated to  
227 temperate conditions (about 10-25 °C). Although the outdoor relative humidity is high in winter, the  
228 indoor absolute humidity hardly changes after artificial calefaction mechanisms. As a consequence,  
229 the indoor ambient is warm and dry, which are benign conditions for virus transmission under  
230 respiratory droplet or aerosol route mechanisms (Schaffer et al., 1976; Soebiyanto et al., 2015).  
231 Warm and dry indoor conditions affect positively the transport of respiratory droplets. In fact, stable  
232 respiratory droplets under low absolute humidity and warm temperature has typical diameter < 5  
233 µm, which remain airborne for prolonged periods (Tellier, 2009). Besides, small aerosol droplets  
234 within the microns range moves randomly, increasing the distance and exposure time over which  
235 transmission can occur. In this way, Figure 5.c suggest that the high transmission rate of 2019-  
236 nCoV in Wuhan at low temperatures (less than about 8 °C), China could be explained from an  
237 increase of indoor human activity, which is realized under regulated ambient conditions  
238 characterized by warm temperature and low absolute humidity, which facilitate virus transmission.  
239 The relatively high dispersion of the data points in Figure 5.c for low temperature might be linked  
240 to confounding factors, including precipitation, air pollution and improvements in medical facilities.  
241 However, a major effect of the meteorological temperature cannot be ruled out. Whether or not the



242 results found in this study can be extended to other cities is an issue that should be addressed in  
243 order to pursue public policies to mitigate and contend with the virus spreading. For instance,  
244 mathematical modeling has suggested that persistent and strict self-isolation is recommended for  
245 cutting off transmission channels (Tang et al., 2020). Under the hypothesis of indoor crowding  
246 effect, a further recommendation involves the development of improved calefaction and air  
247 conditioning equipment for controlling both temperature and absolute humidity. The use of  
248 traditional calefaction and air conditioning devices could be accompanied by humidity controls to  
249 avoid absolute and relative humidity depletion, and in this way reduce the risk of virus  
250 transmission. However, the task temperature and humidity ranges are still unclear. Bu et al. (2020)  
251 studied SARS data and arrived to the conclusion that persistent warm and dry weather is conducive  
252 to the survival of the 2019-nCoV and postulated that temperature ranging 13-19 °C and humidity  
253 ranging 50-80% are suitable conditions for the survival and transmission of coronavirus.

254

## 255 **7. Conclusions**

256 Predicting the transmission dynamics of 2019-nCoV is of prime importance for a proper design of  
257 public health policies intended for disease prevention and control measures as well as for  
258 economical and medical resource allocation. The present study found insights that the  
259 environmental temperature plays an important role in the transmission rate of the 2019-nCoV. It  
260 was postulated that the indoor crowding effect is the main responsible of the high transmission rate  
261 of 2019-nCoV in Wuhan, China in the period January-February 2020.

262

## 263 **Financial Funding**

264 No external financial sources were received for conducting the present study

265

## 266 **Conflict of Interest**

267 No conflict of interest is declared by the authors

268

## 269 **References**

- 270 Backer, J. A., Klinkenberg, D., & Wallinga, J. (2020). Incubation period of 2019 novel coronavirus  
271 (2019-nCoV) infections among travelers from Wuhan, China, 20-28 January 2020.  
272 *Eurosurveillance*, 25(5). doi.org/10.2807/1560-7917.ES.2020.25.5.2000062.
- 273 Hu, Z., Ge, Q., Jin, L., & Xiong, M. (2020). Artificial intelligence forecasting of covid-19 in  
274 china. arXiv preprint arXiv:2002.07112. Retrieved March 18, 2020.

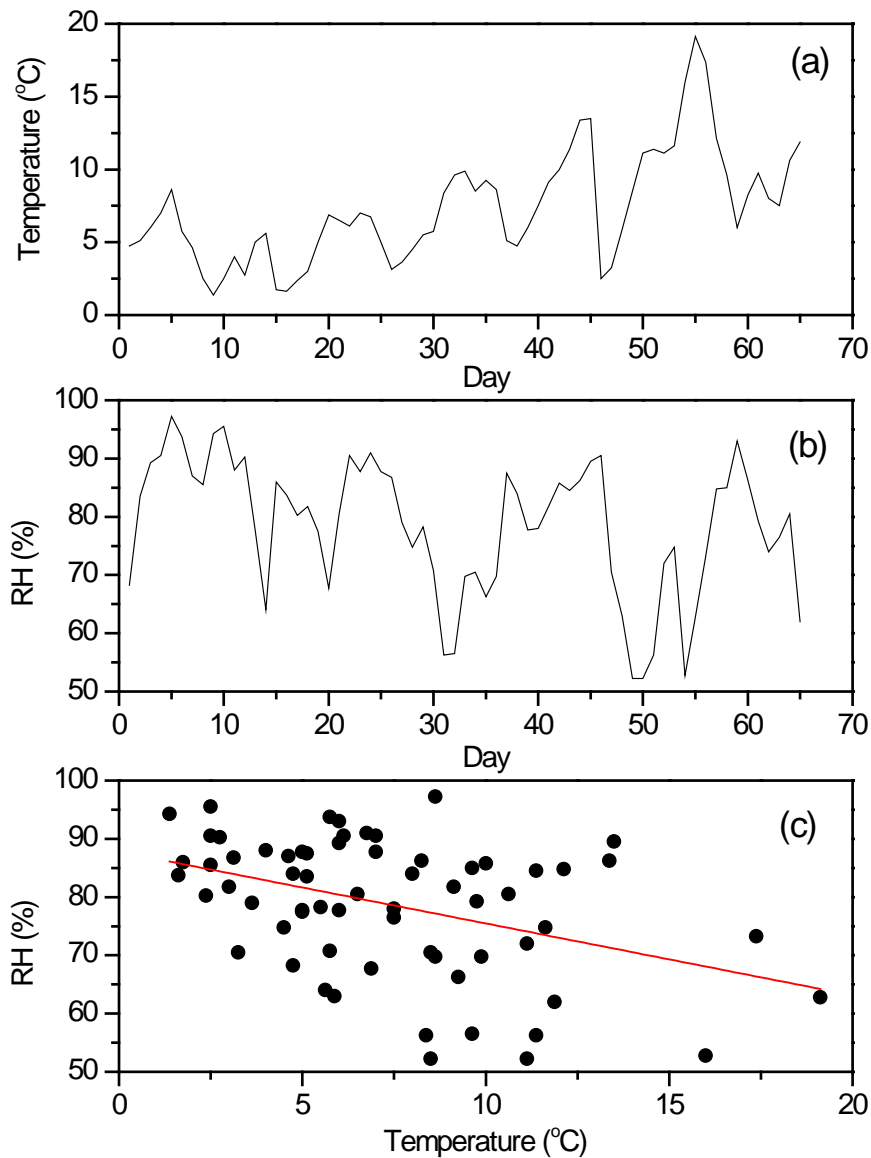
- 275 Lowen, A. C., & Steel, J. (2014). Roles of humidity and temperature in shaping influenza  
276 seasonality. *Journal of Virology*, 88(14), 7692-7695. doi.org/10.1128/JVI.03544-13.
- 277 Oliveiros, B., Caramelo, L., Ferreira, N. C., & Caramelo, F. (2020). Role of temperature and  
278 humidity in the modulation of the doubling time of COVID-19 cases. medRxiv.  
279 doi.org/10.1101/2020.03.05.20031872.
- 280 Peci, A., Winter, A. L., Li, Y., Gnaneshan, S., Liu, J., Mubareka, S., & Gubbay, J. B. (2019).  
281 Effects of absolute humidity, relative humidity, temperature, and wind speed on influenza  
282 activity in Toronto, Ontario, Canada. *Appl. Environ. Microbiol.*, 85(6), doi.org/e02426-18.  
283 10.1128/AEM.02426-18.
- 284 Pica, N., Chou, Y. Y., Bouvier, N. M., & Palese, P. (2012). Transmission of influenza B viruses in  
285 the guinea pig. *Journal of Virology*, 86(8), 4279-4287. doi.org/10.1128/JVI.06645-11.
- 286 Pica, N., & Bouvier, N. M. (2014). Ambient temperature and respiratory virus infection. *The*  
287 *Pediatric Infectious Disease Journal*, 33(3), 311-313. doi.org/10.1097/  
288 INF.0000000000000235.
- 289 Sajadi, M. M., Habibzadeh, P., Vintzileos, A., Shokouhi, S., Miralles-Wilhelm, F., & Amoroso, A.  
290 (2020). Temperature and latitude analysis to predict potential spread and seasonality for  
291 COVID-19. Available at SSRN 3550308. Retrieved March 18, 2020.
- 292 Schaffer, F. L., Soergel, M. E., & Straube, D. C. (1976). Survival of airborne influenza virus:  
293 effects of propagating host, relative humidity, and composition of spray fluids. *Archives of*  
294 *Virology*, 51(4), 263-273. doi.org/10.1007/BF01317930.
- 295 Shen, C. (2015). Analysis of detrended time-lagged cross-correlation between two nonstationary  
296 time series. *Physics Letters A*, 379(7), 680-687. doi.org/10.1016/j.physleta.2014.12.036.
- 297 Soebiyanto, R. P., Gross, D., Jorgensen, P., Buda, S., Bromberg, M., Kaufman, Z., ... & Kiang, R.  
298 K. (2015). Associations between meteorological parameters and influenza activity in Berlin  
299 (Germany), Ljubljana (Slovenia), Castile and Leon (Spain) and Israeli districts. *PloS*  
300 *one*, 10(8). doi.org/10.1371/journal.pone.0134701.
- 301 Steel, J., Palese, P., & Lowen, A. C. (2011). Transmission of a 2009 pandemic influenza virus  
302 shows a sensitivity to temperature and humidity similar to that of an H3N2 seasonal  
303 strain. *Journal of Virology*, 85(3), 1400-1402. doi.org/10.1128/JVI.02186-10.
- 304 Tamerius, J. D., Shaman, J., Alonso, W. J., Bloom-Feshbach, K., Uejio, C. K., Comrie, A., &  
305 Viboud, C. (2013). Environmental predictors of seasonal influenza epidemics across  
306 temperate and tropical climates. *PloS pathogens*, 9(3).

- 307 Tang, B., Bragazzi, N. L., Li, Q., Tang, S., Xiao, Y., & Wu, J. (2020). An updated estimation of the  
308 risk of transmission of the novel coronavirus (2019-nCov). *Infectious Disease Modelling*.  
309 [doi.org/10.1016/j.idm.2020.02.001](https://doi.org/10.1016/j.idm.2020.02.001).
- 310 Tellier, R. (2009). Aerosol transmission of influenza A virus: a review of new studies. *Journal of*  
311 *the Royal Society Interface*, 6(suppl\_6), S783-S790. [doi.org/10.1098/rsif.2009.0302.focus](https://doi.org/10.1098/rsif.2009.0302.focus).
- 312 Tian, S., Hu, N., Lou, J., Chen, K., Kang, X., Xiang, Z., ... & Chen, G. (2020). Characteristics of  
313 COVID-19 infection in Beijing. *Journal of Infection*. [doi.org/10.1016/j.jinf.2020.02.018](https://doi.org/10.1016/j.jinf.2020.02.018).
- 314 Wang, F., Yang, Z., & Wang, L. (2016). Detecting and quantifying cross-correlations by analogous  
315 multifractal height cross-correlation analysis. *Physica A*, 444, 954-962.  
316 [doi.org/10.1016/j.physa.2015.10.096](https://doi.org/10.1016/j.physa.2015.10.096).
- 317 Wang, M., Jiang, A., Gong, L., Luo, L., Guo, W., Li, C., ... & Chen, Y. (2020a). Temperature  
318 significant change COVID-19 Transmission in 429 cities. medRxiv. Retrieved 8 March 2020.
- 319 Wang, J., Tang, K., Feng, K., & Lv, W. (2020b). High temperature and high humidity reduce the  
320 transmission of COVID-19. Available at SSRN 3551767. Retrieved 8 March 2020.  
321 <https://doi.org/10.1101/2020.02.22.20025791>.
- 322 Zhao, S., Lin, Q., Ran, J., Musa, S. S., Yang, G., Wang, W., ... & Wang, M. H. (2020). Preliminary  
323 estimation of the basic reproduction number of novel coronavirus (2019-nCoV) in China,  
324 from 2019 to 2020: A data-driven analysis in the early phase of the outbreak. *International*  
325 *Journal of Infectious Diseases*. 92, 214-217. [doi.org/10.1016/j.ijid.2020.01.050](https://doi.org/10.1016/j.ijid.2020.01.050).
- 326 Zhu, N., Zhang, D., Wang, W., Li, X., Yang, B., Song, J., ... & Niu, P. (2020). A novel coronavirus  
327 from patients with pneumonia in China, 2019. *New England Journal of Medicine*. 382, 727-  
328 733. [doi.org/10.1056/NEJMoa2001017](https://doi.org/10.1056/NEJMoa2001017).
- 329
- 330
- 331
- 332

333

334

335



336

337 **Figure 1.** (a) Mean daily meteorological temperature, and (b) relative humidity (RH) in Wuhan,  
338 China for the period from 1 January to 6 March, 2020. (c) Plot of the relative humidity versus  
339 temperature, showing negative correlations ( $\rho = -0.42$ ).

340

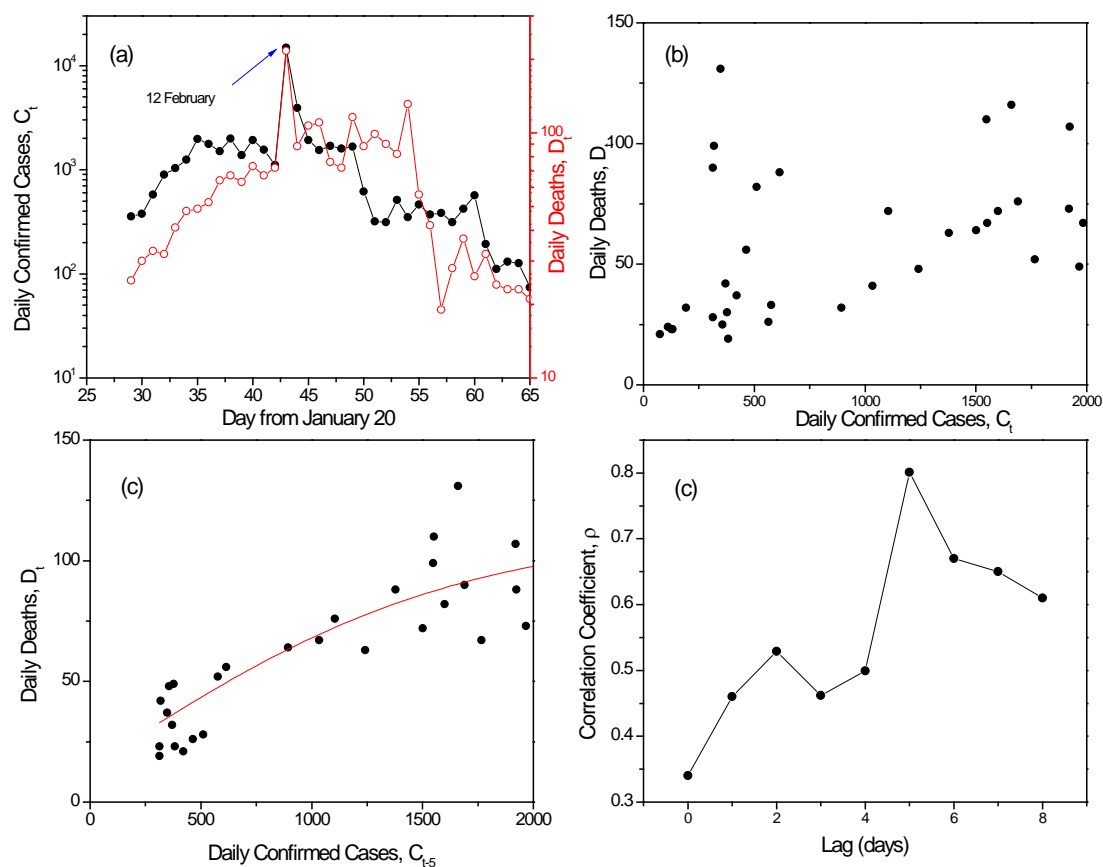
341

342

343

344

345



346

347

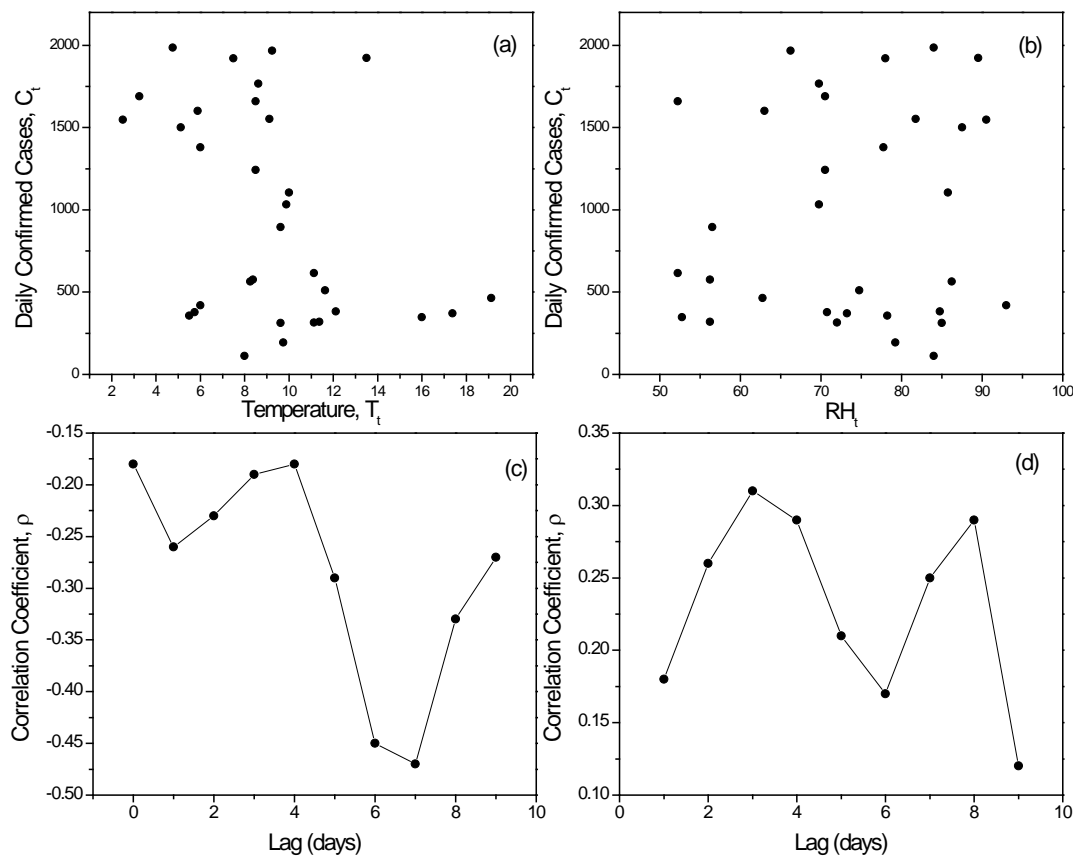
348 **Figure 2.** (a) Number of daily confirmed and death cases in Wuhan, China, for the period from 1  
349 January to 6 March, 2020. The large peak in 12 February corresponds to improvements in the  
350 detection methods. (b) Plot of contemporaneous daily deaths ( $D_t$ ) versus daily confirmed ( $C_t$ ) cases.  
351 (c) Plot of daily deaths ( $D_t$ ) with respect to 5-days lagged daily confirmed cases ( $C_{t-5}$ ). (d) Behavior  
352 of the correlation coefficient with respect to the lag in daily confirmed cases.

353

354

355

356



357

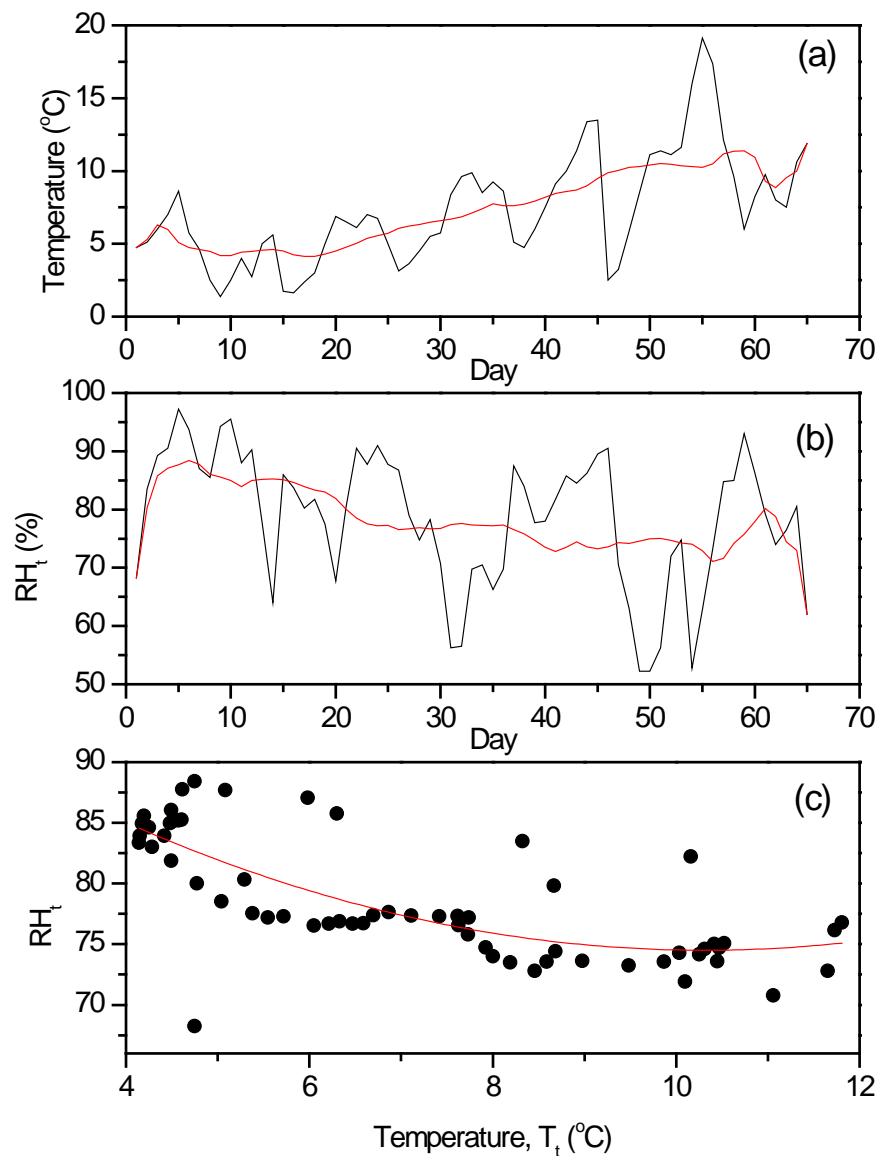
358

359 **Figure 3.** Plots of daily confirmed cases versus (a) temperature and (a) relative humidity. The plots  
360 exhibit a scattered pattern with weak correlations. The behavior of the correlation coefficient with  
361 respect to the lag for (c) temperature and (d) relative humidity exhibit a peak in magnitude for lags  
362 of about 5-8 days.

363

364

365



366

367 **Figure 4.** Meteorological (a) temperature, and (b) relative humidity in Wuhan, China, for the period  
368 from 1 January to March 6, 2020. The red lined depict the long-term trend obtained by 15-days  
369 moving average filtering. (c) Plot of the trend relative humidity and the trend temperature. A  
370 negative correlation between these trends can be observed.

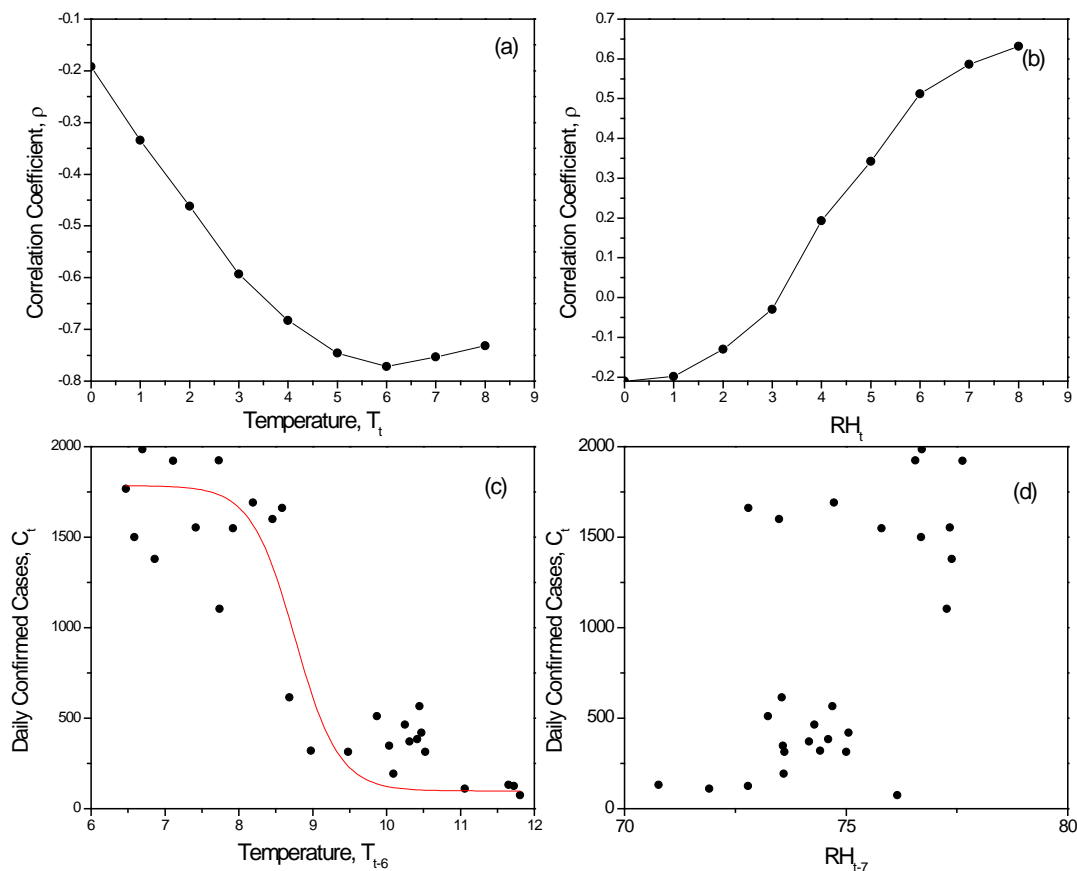
371

372

373

374

375



376

377

378 **Figure 5.** Behavior of the correlation coefficient with respect to the lag, for (a) trend temperature

379 and (b) trend relative humidity. (c) Plot of daily confirmed cases and 6-day lagged trend

380 temperature. (d) Plot of daily confirmed cases and 7-day lagged trend relative humidity.

381

382